MADRID
inter.noise 2019
June 16 - 19
NOISE CONTROL FOR A BETTER ENVIRONMENT

Nonlinear Vibration Demonstration: Clamped Elastic Plate With Dry Sand Loading

Ava Twitty[1]
5568 Carvel St.
Churchton, MD 20733, USA

Murray Korman[2]
United States Naval Academy
Physics Department
572-C Holloway Road
Annapolis, MD 21402, USA

ABSTRACT

Experiments using soil-plate-oscillators (SPO) involve a cylindrical column of granular media (masonry sand) supported by a clamped circular elastic acrylic plate (12.7 cm diam, 3.2 mm thick). The plate is clamped between two 20.3 cm O.D., 12.7 cm I.D., 6.4 cm thick flat toroidal brass "rings." Two 6 inch (15 cm) diameter subwoofers (located 10 cm above the soil) are driven by an amplified swept sinusoidal chirp which drives the soil column (2.5 cm in height). A spectrum analyzer measures the voltage signal from the laser Doppler vibrometer particle velocity vs. frequency near the center of the column's surface. The resonant frequency decreases with increasing amplitude – representing softening in the nonlinear system. The back-bone curve (locus of the resonant frequency f vs. corresponding peak velocity v data points) has a distinct arching shape where the slope of the velocity increases with decreasing frequency. Here the resonant frequency goes from 249 to 227 Hz. A lumped element bilinear hysteresis model appears to describe the shape of the tuning curves and backbone curve. Measurements of the particle velocity across the surface (generated by individual tuning curves at each scan position) are used to construct modal shapes at specific resonant frequencies.

Keywords: Granular Material, Environment, Vibration, Nonlinear, Tuning Curve
I-INCE Classification of Subject Number: 76

1. INTRODUCTION

Non-metallic land mines are difficult to detect using conventional ground penetrating radar detection methods. In some difficult detection scenarios, acoustic landmine detection

[1] avati226@gmail.com
[2] korman@usna.edu

provides some utilization as a confirmation sensor. Understanding the air-borne excitation and vibro-acoustic detection of a complex structural elastic target buried in a soil or roadbed with natural weathered inhomogeneous layered granular media (including debris or shrapnel) is computationally challenging. However, a model apparatus called a soil (sand) plate oscillator SPO is a robust physical model of the nonlinear interaction of granular media (contained in an open cylindrical column). Here, sand is interacting with the vibration of a clamped circular elastic plate which supports the granular column. In this paper, we describe experiments using the SPO apparatus that are similar to experiments performed in acoustic landmine detection. See references [1-13].

The sand plate oscillator (SPO) apparatus consists of two circular brass toroidal shaped flanges sandwiching and clamping a thin circular elastic plate. The apparatus can model the acoustic landmine detection problem. Here, dry sifted masonry sand (a nonlinear mesoscopic elastic granular material) is supported at the bottom by the acrylic plate (12.7 cm clamped diam, 0.318 cm thick, and density 1.18 g/cc) and stiff cylindrical sidewalls of the upper/lower flanges. The upper flange contains a level column of sand (corresponding to burial depth) while the underside of the clamped plate is air-backed. The bottom of the lower flange is fastened to a round steel plate (20.3 cm diam and 2.54 cm thick).

2. EXPERIMENTAL OVERVIEW AND SETUP

Experiments are performed with the sand plate oscillator to (a) to first understand the effects of adjusting the height of the sand column (i.e. adding mass to the system) to determine the relationship between the fundamental resonant frequency versus the mass loading. In this experiment the laser Doppler vibrometer LDV remains fixed at the center of the sand surface which forms a planar circular region. The loud speakers generate a swept tone airborne sound excitation at a fixed constant acoustic pressure amplitude for each tuning curve measurement - corresponding to a sand column of 88, 176, 264, … up to 968 g, respectively. The mass of sand m_s = 968 g corresponds to a final sand column of height 5.5 cm. It is observed that the fundamental frequency initially decreases with adding mass, reaching a minimum value, and then increases with further added mass. Next, in (b) the sand mass is adjusted to m_s = 454 g (a column height 2.5 cm) and LDV measurements are made at 15 equally separated scan positions across the sand surface. Here, the swept tone excitation goes from 50 < f < 2050 Hz over a 79 second sweep time where the dynamic analyzer records the LDV rms voltage signal frequency response of the sweep and stores the digital file to a computer storage location. While keeping the pressure amplitude of the excitation constant, the LDV is positioned at a new location and a new sweep is made to obtain another rms voltage signal frequency response which is recorded and stored. The frequency response files from all scan positions are transferred to Mathematica^{TM} version 9 such that an rms modal analysis (c) can be computed. For each scan position (at a specified frequency) the rms voltage signal is plotted vs. the scan position. This is repeated for the discrete frequencies 50, 55, 60, … ,2050 Hz to obtain an rms voltage signal (proportional to the rms particle velocity vibration) vs. scan position across the sand surface. At particular resonant frequencies, on can observe modes shapes that are closely related to pure radial mode drum-like behavior. Finally in (d) a comparison between the nonlinear tuning curve response (on the center of the sand surface) of the SPO is compared to the nonlinear tuning curve response on the sand surface over an inert VS 1.6 plastic anti-tank mine that is buried 5 cm deep in a 58 cm square sand box (constructed with concrete walls 7 cm thick and 23 cm tall) and placed on a concrete floor.

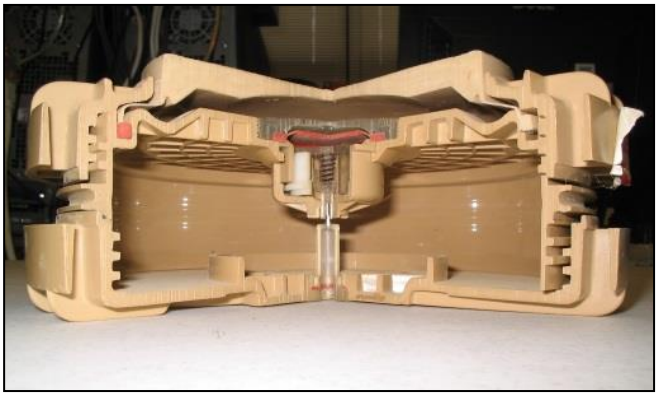

Figure 1. (a) Cross-section of a VS 1.6 Anti-tank plastic landmine. The top-plate diam is 14.5 cm and the overall height is 9.3 cm. The VS 1.6, buried in a roadbed, can be detected using air-borne sound excitation and remote LDV measurements along the soil or gravel surface. (b) The brass soil-plate-oscillator represents an ideal model of some aspects of acoustic landmine detection, where a confined soil column is supported by a clamped 1/8 inch thick acrylic elastic circular plate. The inside diam of the top toroidal flange that clamps the plate with an identical bottom flange is 5.0 inches. The small magnet and AC coil were not used in the experiments reported here.

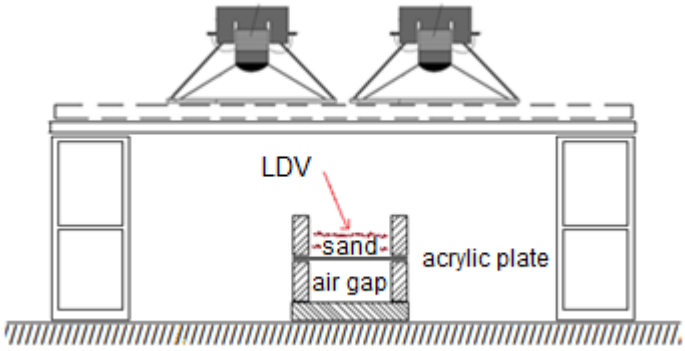

Figure 2. Soil plate oscillator with sand loading is driven by airborne sound generated from two loud speakers. The laser Doppler vibrometer LDV signal going to an Agilent 356701A dynamic analyzer measures the particle velocity response vs. frequency at 15 scan positions across the sand interface. The speakers are driven from separate constant current amplifiers driven from the swept tone output of the analyzer.

Figure 1(a), (b) show a cross-section of a VS 1.6 anti-tank plastic landmine and SPO respectively, while Figure 2 shows the experimental setup. Figure 3(a) shows the SPO with sand loading and reflective discs, while Fig. 3(b) shows the LDV in scan mode along with the two 6.5 inch and loudspeaker placed 20 cm above the sand surface. Individual speakers are driven using separate constant current amplifiers.

Figure 3. (a) Close-up of the soil plate oscillator SPO with 445 grams of sand loading (density 1.43 g/cc). The upper toroidal brass flange is 5.0 inch I.D., 8.0 inch O.D. and 2.5 inch tall. Reflective 0.6 cm diam disks (1 mm thick) are placed along the sand surface to allow excellent reflection by the Polytec 100 laser Doppler vibrometer. (b) Experimental setup of SPO being driven by airborne sound generated from two 6.5 inch diam, 8 Ω loud speakers. LDV measures the sand particle velocity response vs. frequency at 15 scan locations across the sand surface.

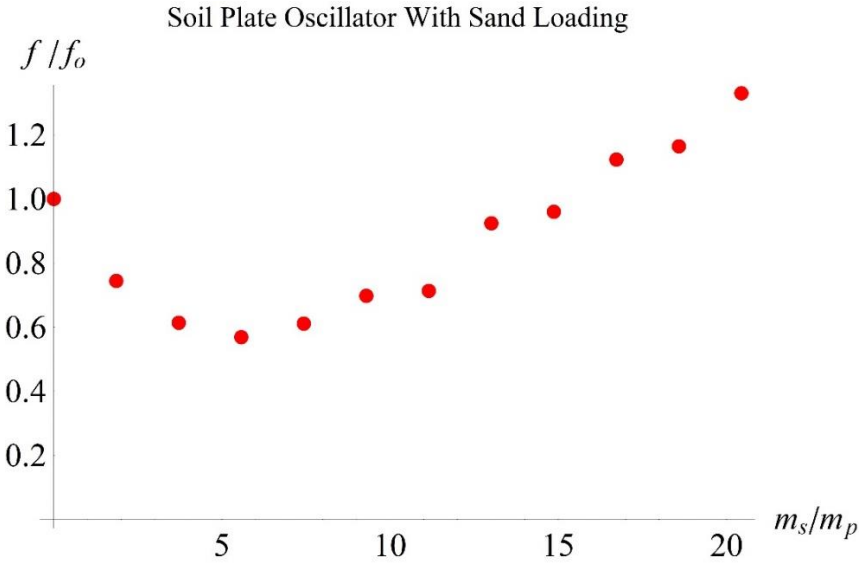

Figure 4. The SPO fundamental resonant frequency f vs. sand mass loading m_s .

In Figure 4 we measure the resonant frequency vs. soil mass loading. LDV tuning curves for the SPO are measured on the center of the sand with a constant air-borne radiated sound pressure amplitude for each of the 12 tuning curve sweeps from $50 < f < 850$ Hz. Here, $f_o = 414$ Hz is the resonant frequency with no sand loading, and $m_p = 47.4$ grams is the clamped mass (5 inch diam) of the acrylic plate. The physical size of the acrylic plate was 1/8 inch thick and 8 inches in diameter. This matches the outer diameter of the 8 inch OD brass toroidal flanges, which are 5 inch ID and 2 inch thick. In particular for $m_s = 445$ g , the resonant frequency $f \sim 240$ Hz .

3. EXPERIMENTAL RESULTS

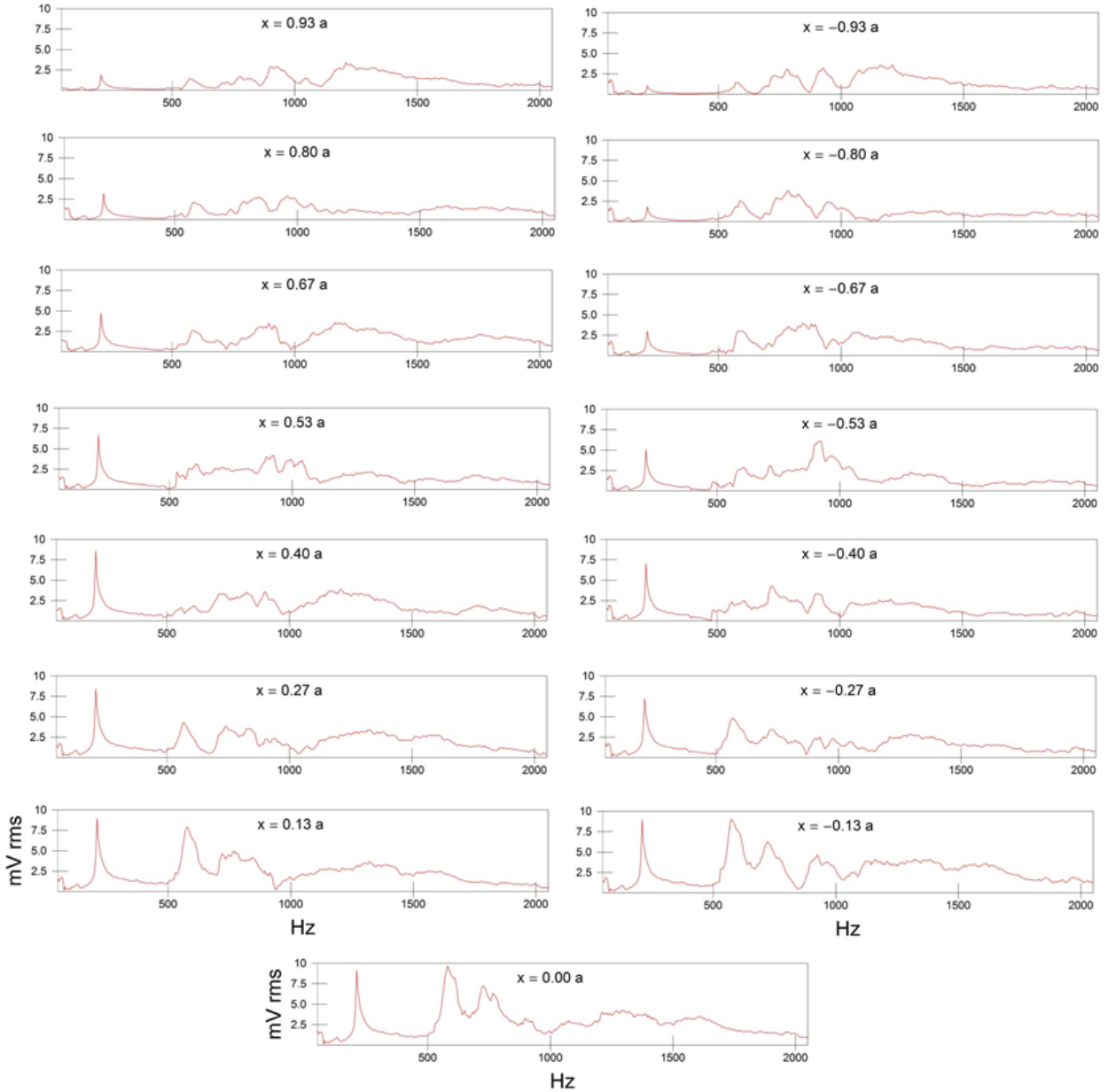

Figure 5. LDV soil-surface vibration voltage response vs. frequency, at 15 scan positions across the sand interface of the SPO. In the "swept sinusoid" instrument mode of the dynamic spectrum analyzer, the source output sweeps from 50 < f < 2050 Hz (in 79 seconds) for each scan position. Vertical scale: 10 mV rms corresponds to an rms particle velocity of 250 micro meters/second. The scan position is labeled by x where $-a < x < a$ and $a = 2.5$ inches is the radius of the clamped elastic plate (which supports the cylindrical sand column).

In Figure 5, above, voltage vs. frequency response curves are measured at 15 scan positions across the sand interface in an effort to measure the soil-surface vibration response vs. scan position at a fixed frequency. Evidence of a strong modal response at f ~ 215 Hz can readily be observed from the 15 voltage vs. frequency response curves shown above.

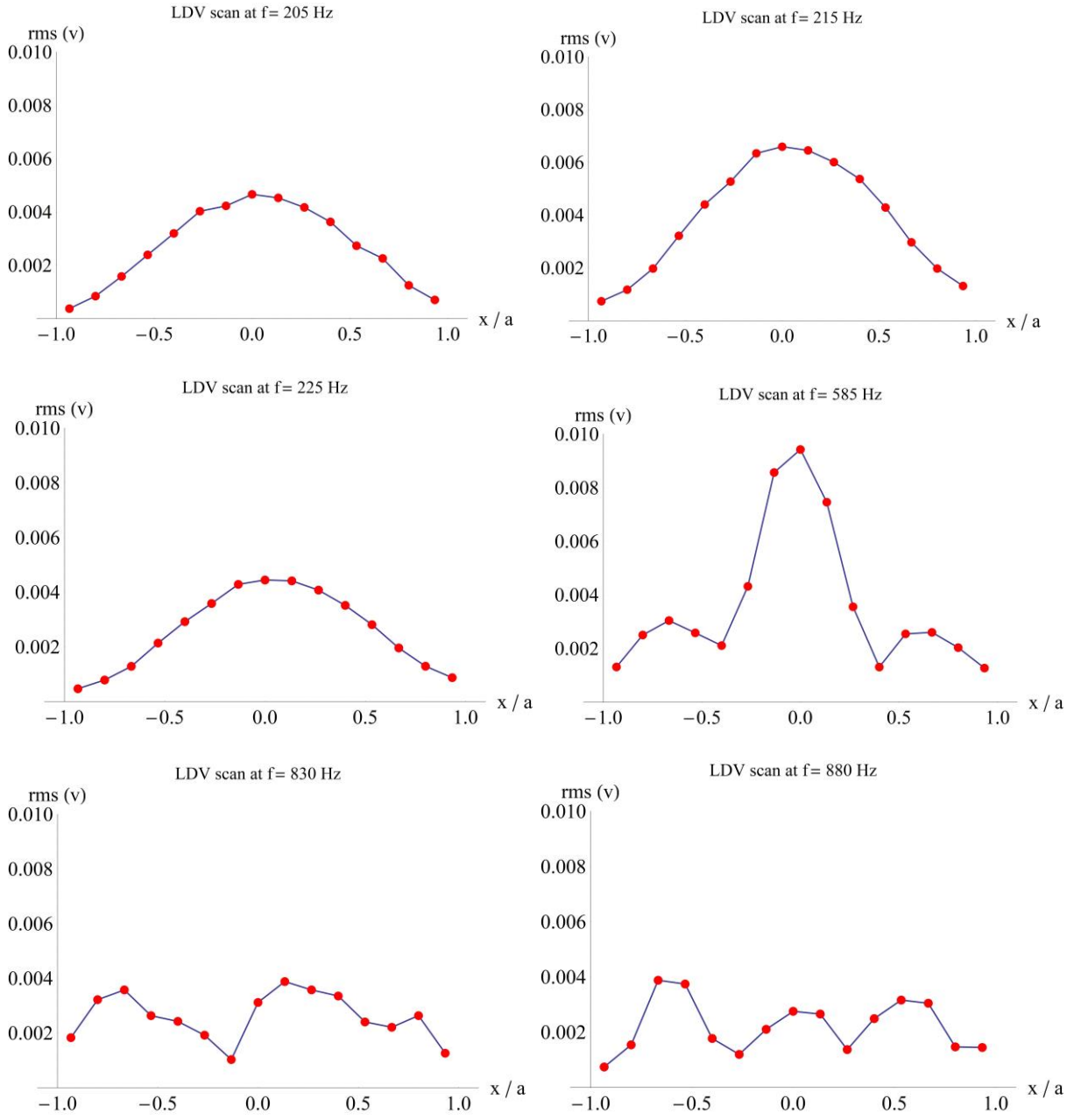

Figure 6: Sand plate oscillator mode shapes. Top left, f =205 Hz; Top right, f =215 Hz; and Middle left, f = 225 Hz, exhibit the lowest radial mode shape near the resonant frequency of 215 Hz. Middle right, f = 585 Hz, exhibits the second lowest radial mode shape. Bottom left, f = 830 Hz, exhibits a possible mode shape that does not have azimuthal symmetry. Bottom right, f = 880 Hz, exhibits a possible mode shape where the peak at the center is less than the two side peaks.

Figure 6 shows the lowest mode near 215 Hz, along with more complicated modes at 585, 830 and 880 Hz.

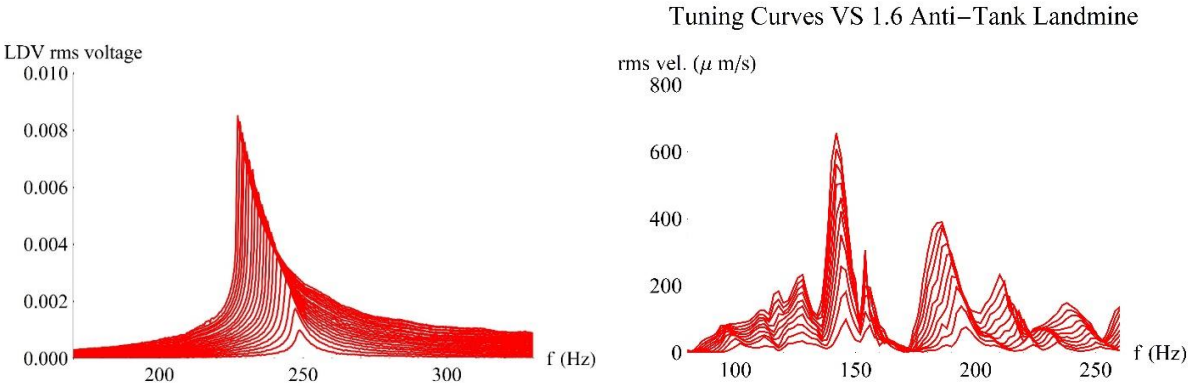

Figure 7. (a) SPO (5 inch diam clamped acrylic plate 1/8 inch thick) with 1 inch dry sifted masonry sand (m_s ~ 445 g). LDV tuning curves on the center of the sand surface. For each of the tuning curve sweeps from 100 < f < 400 Hz, use a uniform incremental increase in the air-borne radiated sound pressure. Vertical scale: 10 mVrms corresponds to 250 μ m/s. (b) On the surface (over the mine) tuning curve particle velocity vs. frequency response for the VS 1.6 buried 2 inches deep in dry sifted masonry sand in a large open sand tank.

A comparison of the nonlinear tuning curve response using the SPO (with a 2.5 cm sand column) with the VS 1.6 inert anti-tank plastic landmine (buried 5 cm below the sand surface) reveals some similarities as well as some differences. The VS 1.6 has resonant peaks near 150, 200, and 250 Hz which exhibit frequency "softening" (lower resonant frequency response at higher drive amplitudes). In particular, the VS 1.6 250 Hz resonant frequency shifts to about 235 Hz over a span of 200 μ m/s soil particle velocity. In comparison, the SPO 250 Hz resonant peak appears to shift by $0.85 \times 250\ \mu\ m/s \sim 210\ \mu\ m/s$. A "backbone" curve defined by the coordinates of the resonant frequency and associated peak value for the particle velocity show a slight arching in the SPO case near 250 Hz. There is also some backbone curvature near the 145 Hz peak of the VS 1.6 . The slight arching in the backbone curve can be predicted using Caughey's bilinear hysteresis lumped element model [14] of a forced harmonic oscillator.

6. CONCLUSIONS

The soil plate oscillator experiments involved measurement of the fundamental resonant frequency vs. mass loading effects can be explained by modelling the SPO as a lumped element with mass loading of the oscillator by a thin cylindrical disk. For small loading the disk is flexible and the effective spring constant of the disk will be comparably small. But for significant mass loading the disk effective spring constant will dominate the mass loading, such that the frequency of the SPO will start to increase [10]. In LDV scans across the sand surface the particle velocity frequency response vs. frequency is recorded at 15 scan positions across the SPO's sand surface. The results are utilized to compute modes shapes at particular resonant frequencies. Some of the recognized mode shapes look like drum-like radial modes while others suggest a lack of azimuthal symmetry. In nonlinear tuning curve experiments, the LDV is placed on the sand surface at the center of the SPO. Here, tuning curves exhibit "softening" as the drive amplitude increases. Further the backbone curve exhibits a linear fit or a slightly arched

behaviour. A linear backbone curve can be described by mesoscopic nonlinear elastic behaviour - similar to the resonant tuning curve behaviour observed in geo-materials like sand stone [15]. With further increase in drive amplitude the tuning curve exhibits a slightly arched or curvature behaviour. This behaviour can be predicted by using a bilinear hysteresis lumped element model [14] in a driven harmonic oscillator. Comparisons of the SPO tuning curves with a buried VS 1.6 inert plastic anti-tank landmine in a sand tank are reasonable and offer some insight on the future use of the SPO to model acoustic landmine detection using airborne sound.

7. ACKNOWLEDGEMENTS

The authors wish to thank the Physics Department at the United States Naval Academy for the opportunity and resources to do this research. In particular the authors wish to thank Mr. Gary Bishop, Mr. Patrick Meyers and Ms. Rebecca Carr for their technical support. In particular we give special thanks to Mr. Jeff Walbert for expert machining of various components of the apparatus. It was former Midshipman Kathleen Pauls (2007) who designed the brass toroidal soil plate oscillator.

8. REFERENCES

The following selected references should be helpful to the reader for further background on the research.

1. J. M. Sabatier and N. Xiang, "An investigation of a system that uses acoustic-to-seismic coupling to detect buried anti-tank landmines," IEEE Trans. Geoscience and Remote Sensing 39, 1146-1154 (2001).

2. N. Xiang and J. M. Sabatier, "An experimental study on antipersonnel landmine detection using acoustic-to-seismic coupling," J. Acoust. Soc. Am. **113**, 1333-1341 (2003).

3. D. M. Donskoy, "Nonlinear vibro-acoustic technique for land mine detection", SPIE Proc. **3392**, 211-217 (1998); "Detection and discrimination of nonmetallic land mines," SPIE Proc. **3710**, 239-246 (1999).

4. M. S. Korman and J. M. Sabatier, "Nonlinear acoustic techniques for landmine detection," J. Acoust. Soc. Am. **116**, 3354-3369 (2004).

5. D. M. Donskoy, "Nonlinear vibro-acoustic technique for land mine detection", in *Detection and Remediation Technologies for Mines and Minelike Targets III*, ed. by A. C. Dubey, J. F. Harvey and J. T. Broach, SPIE Proc. **3392**, 211-217 (1998); "Detection and discrimination of nonmetallic land mines," in *Detection and Remediation.*

6. D. M. Donskoy, A. Ekimov, N. Sedunov, and M. Tsionskiy, "Nonlinear seismo-acoustic land mine detection and discrimination," J. Acoust. Soc. Am. **111**, 2705-2714 (2002).

7. D. M. Donskoy, "Nonlinear seismo-acoustic landmine detection." J. Acoust. Soc. Am. **123** (5), 3042 (2008).

8. W. C. Alberts, J. M. Sabatier and R. Waxler, "Mechanical resonances in the low-frequency vibration spectrum of a cylindrically symmetric, anti-tank landmine," J. Acoust. Soc. Am. **123** (5), 3044 (2008).

9. M. S. Korman, J. M. Sabatier, K. E. Pauls and S A. Genis, "Nonlinear acoustic landmine detection: comparison of off-target soil background and on-target soil-mine nonlinear effects," SPIE Proceedings Volume 6217, Detection and Remediation Technologies for Mines and Minelike Targets XI; 62170Y (2006).

10. M. S. Korman, D. V. Duong and A. E. Kalsbeck, "Electrodynamic soil plate oscillator: Modeling nonlinear mesoscopic elastic behavior and hysteresis in nonlinear acoustic landmine detection," AIP Conference Proceedings, Volume 1685, Issue 1, id.080003, 20th ISNA, Écully, France (29 June – 3 July 2015).
11. E. V. Santos and M. S. Korman, "Nonlinear tuning curve vibration using a column of non-wetted or wetted glass beads vibrating over a clamped elastic plate: Case for airborne excitation," J. Acoust. Soc. Am. 144 (3) Pt. 2, p. 1856 (2018).
12. F. M. Browne and M. S. Korman, "Experiments in linear and nonlinear acoustic landmine detection." J. Acoust. Soc. Am. 144 (3) Pt. 2, p. 1856 (2018).
13. J. M. Cartron and M. S. Korman, "Demonstration of acoustic landmine detection using a clamped soil plate oscillator with airborne sound excitation." J. Acoust. Soc. Am. 144 (3) Pt. 2, p. 1856 (2018).
14. T. K. Caughey, "Sinusoidal excitation of a system with bilinear hysteresis," Transactions of the ASME, J. of Applied Mech., **27**, 640-643 (1960).
15. L. A. Ostrovsky and P. A. Johnson, "Dynamic nonlinearity elasticity in geomaterials, "Rivista Del Nouvo Cinmento, **24**, serie 4, No. 7, 1-46 (2001).